Structure of ^{60,62}Fe and the onset of $\nu g_{9/2}$ occupancy

N. Hoteling,[1,2,*] C. J. Chiara,[1,2,†] R. Broda,[3] W. B. Walters,[1] R. V. F. Janssens,[2] M. Hjorth-Jensen,[4] M. P. Carpenter,[2] B. Fornal,[3] A. A. Hecht,[1,2,‡] W. Królas,[3,5] T. Lauritsen,[2] T. Pawłat,[3] D. Seweryniak,[2] X. Wang,[2,6,§] A. Wöhr,[1,2,6] J. Wrzesiński,[3] and S. Zhu[2]

[1]*Department of Chemistry and Biochemistry, University of Maryland, College Park, Maryland 20742, USA*

[2]*Physics Division, Argonne National Laboratory, Argonne, Illinois 60439, USA*

[3]*Niewodniczański Institute of Nuclear Physics PAN, Radzikowskiego 152, PL-31-342 Kraków, Poland*

[4]*Department of Physics and Center of Mathematics for Applications, University of Oslo, N-0316 Oslo, Norway*

[5]*Joint Institute for Heavy Ion Research, Oak Ridge, Tennessee 37831, USA*

[6]*Department of Physics, University of Notre Dame, Notre Dame, Indiana 46556, USA*

(Received 28 May 2010; published 7 October 2010)

Level structures in $^{60,62}Fe_{34,36}$ and adjacent nuclei were studied with Gammasphere using the reaction of a 430-MeV ^{64}Ni beam on a 55-mg/cm^2 thick ^{238}U target. High-spin level schemes were deduced from singly- and doubly-gated prompt coincidence events. Levels populated in the β decay of ^{60,62}Mn isomers were studied in singly- and doubly-gated delayed coincidences. Spin and parity assignments were deduced from angular correlations of γ rays observed in both nuclei, leading to firm positive-parity yrast assignments up through 8^+ in ^{62}Fe. The observed levels for ^{60}Fe up to ~3.5 MeV compare well with pf shell-model calculations available in the literature. Calculations performed in a limited pfg basis exhibit reasonable agreement for the 2^+, 4^+, and 6^+ levels in ^{62}Fe. However, theoretical descriptions that include the newly identified negative-parity levels in ^{62}Fe require a much larger basis, necessarily including $g_{9/2}$ neutrons, as well as improved interactions leading to negative-parity levels.

DOI: 10.1103/PhysRevC.82.044305 PACS number(s): 23.20.Lv, 23.20.En, 21.60.Cs, 27.50.+e

I. INTRODUCTION

The structure of neutron-rich iron nuclei has been the subject of considerable interest in recent years, in part because of the discovery of a downward trend in the 2_1^+ energies for $^{64,66}_{26}Fe_{38,40}$ and a rise in $B(E2; 2^+ \rightarrow 0^+)$ strengths as neutron number 40 is approached [1–3]. This behavior is in sharp contrast to that seen in the even-even Ni isotopes when moving toward $^{68}_{28}Ni_{40}$ [4]. A similar trend of decreasing 2_1^+ energies unfolds in the $_{24}$Cr isotopes and has given rise to much discussion, mostly in terms of the possible onset of deformation [5,6]. To better understand the role that the $g_{9/2}$ neutron orbital plays in these intriguing trends, several attempts have been made to reproduce this behavior by implementing large-scale shell-model calculations with this $g_{9/2}$ orbital included in the model space [7–10]. However, large dimensionality makes such calculations difficult, and truncations are often necessary. Another challenge lies in the determination of two-body matrix elements associated with $g_{9/2}$ neutron configurations, as little information is available for most neutron-rich nuclides at the edge of the pf shell, below $Z = 28$. Thus, it is especially important to establish new level structures beyond the 2^+ energies and to provide a more solid basis for the proposed spin and parity assignments for as many neutron-rich nuclei of this region as possible. In the present work, revised and expanded level schemes are proposed for ^{60,62}Fe on the basis of coincidence and angular-correlation data following the decay of ^{60,62}Mn isomers, as well as on the basis of reactions populating levels in these iron isotopes directly.

II. PREVIOUS STUDIES

The structure of ^{60}Fe was studied by Norman *et al.* [11], who proposed 4^+, 2^+, and $(3)^+$ spin and parity for levels at 2114, 2299, and 2792 keV, respectively, populated in the decay of a 1.7-s high-spin ^{60}Mn isomer. Liddick *et al.* [12] subsequently studied the decay of a 280-ms low-spin isomer in ^{60}Mn and observed population of the two 0^+ levels at 1974 and 2356 keV, previously identified in (t, p) reaction studies [13]. Liddick *et al.* [12] also argued that the low- and high-spin isomers in ^{60}Mn most likely have spins and parities of 1^+ and 4^+, respectively, based on the observed β-decay feeding intensities and the known $M3$ transition linking the two long-lived states [14]. In addition to these low-spin studies, extensive high-spin structure has been recently reported for ^{60}Fe by Deacon *et al.* following a fusion-evaporation reaction [15].

The structure of ^{62}Fe was studied by Runte *et al.* [16] following β decay of ^{62}Mn. In that work, the authors proposed the first 2^+ and 4^+ states. Later, the level scheme was extended up to medium spin in two deep-inelastic reaction experiments [17,18]. Further confirmation of some of the levels proposed from those experiments was recently provided by Lunardi *et al.* [7], but ambiguity remains for a number of spin and parity assignments. Runte *et al.* [16] reported a single half-life of 880(150) ms for the β decay of a proposed (3^+)

*Present address: Los Alamos National Laboratory, Los Alamos, New Mexico 87545, USA.

†Corresponding author.

‡Present address: Department of Chemical and Nuclear Engineering, University of New Mexico, Albuquerque, New Mexico 87131-0001, USA.

§Present address: Department of Physics, Florida State University, Tallahassee, Florida 32306-4350, USA.

level in ^{62}Mn. A more precise value of 671(5) ms was given in Ref. [1], and a separate component with a half-life of 84(10) ms was also identified [19]. The presence of both isomers was confirmed in the recent work of Gaudefroy *et al.* [20], where two components with half-lives 92(13) and 625 ms were reported. These authors also studied the decay of the 209-ms 0^+ ground state in ^{62}Cr and concluded that the spin and parity assignment for the shorter-lived ^{62}Mn isomer must be 1^+.

Consequently, ^{58,60,62}Mn all exhibit β decay from a low-spin 1^+ level that has been established as the ground state in ^{58,60}Mn. As $M3$ transitions have been observed in the decay of the higher-spin isomers in ^{58,60}Mn, a 4^+ spin and parity assignment was established for these long-lived states in these two nuclei. As noted, 1^+ quantum numbers have also been established for the short-lived ^{62}Mn isomer. The relative positions of the two β-decaying isomers in ^{62}Mn have not been determined, nor have the spin and parity of the longer-lived state. However, only a separation of a few keV would permit the higher-spin isomer to have 3^+ quantum numbers. Thus, we propose a tentative (4^+) assignment for the higher-spin isomer in ^{62}Mn in analogy with the lower-mass Mn isotopes.

III. EXPERIMENTAL PROCEDURES

Excited states in ^{60,62}Fe were populated with the ^{64}Ni + ^{238}U reaction at 430 MeV using a 55-mg/cm^2 target located at the center of the Gammasphere array [21], which was configured with 100 Compton-suppressed high-purity Ge detectors. The ^{64}Ni beam was delivered by the Argonne Tandem Linac Accelerator System at Argonne National Laboratory in pulses separated by 410 ns. Multifold γ-ray coincidence events requiring a minimum of three γ rays were recorded [22]. The data were sorted in terms of the time with respect to a given beam burst, so that four three-dimensional coincidence histograms (*cubes*) could be constructed. These included the prompt (PPP) and delayed (DDD) coincidence cubes, which are discussed here. Events in the PPP cube must include γ rays detected within a 40-ns window centered around the beam pulse. Included in the DDD cube are γ rays arising from the radioactive or isomeric decay of the nuclei produced in the nuclear reactions that occur within 40 ns of each other, but outside of the 40-ns window for prompt events. (A small contribution from long-lived decay events will also be present as background in the PPP cube, but this is dominated by the prompt events.) Further details regarding the experiment, including the derivation of these cubes, are given in Refs. [2,22].

IV. RESULTS

A. ^{62}Fe level scheme

Coincidence spectra with a double gate on the 877- and 1299-keV γ-ray transitions in ^{62}Fe in the PPP and DDD cubes are illustrated in Figs. 1(a) and 1(b), respectively. Peaks associated with all of the prompt γ rays reported in Refs. [7,17,18] are confirmed in Fig. 1(a). The delayed spectrum in Fig. 1(b), when compared to the similarly gated prompt spectrum in Fig. 1(a), illustrates the sensitivity achieved for distinguishing between the prompt and delayed decay schemes for a given nucleus. Here, the delayed ^{62}Fe γ rays follow the β decay of ^{62}Mn.

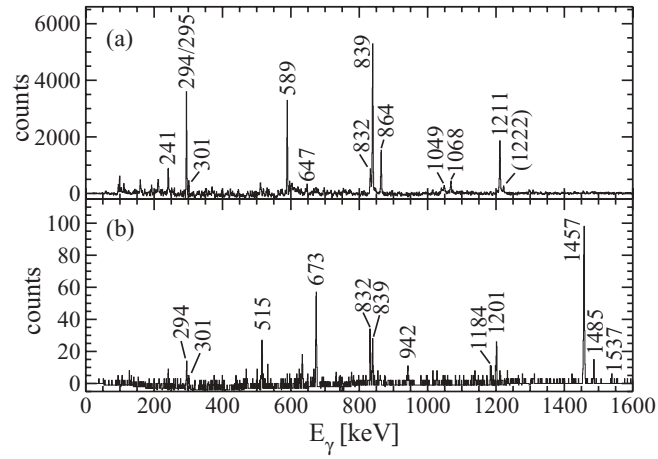

FIG. 1. Coincidence spectra double-gated on the 877- and 1299-keV transitions in the (a) PPP and (b) DDD data. The γ rays assigned to ^{62}Fe are labeled with their energies in keV.

The spectrum from a double gate in the PPP cube on the 839- and 1299-keV γ rays is given in Fig. 2, where new transitions at 647, 754, 1049, and 1297 keV, and tentatively at 1222 keV, are present. Additionally, the spectrum from a double gate on the 877- and 1814-keV γ rays in Fig. 3 provides evidence for lines at 301 keV (weakly) and at 317 keV. These coincidence relationships were used to generate the new level scheme for the prompt γ rays proposed in Fig. 4. Properties of the levels and γ rays assigned to ^{62}Fe are listed in Table I, in which the six newly identified transitions are underlined. The observed coincidence relationships support the placement of the proposed new levels at 4359 and 4902 keV and the 317-keV line depopulating the level at 3009 keV. The peak for the 1068-keV γ ray depopulating the state at 5319 keV

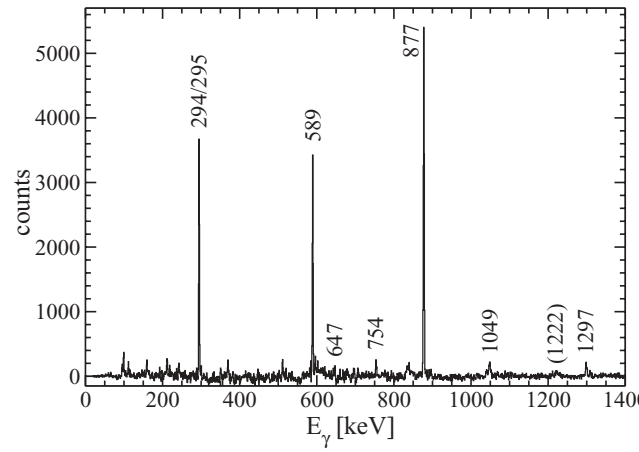

FIG. 2. Coincidence spectrum double-gated on 839- and 1299-keV transitions in the PPP data. The γ rays assigned to ^{62}Fe are labeled with their energies in keV. The 1222-keV line is tentative and is, thus, labeled in parentheses.

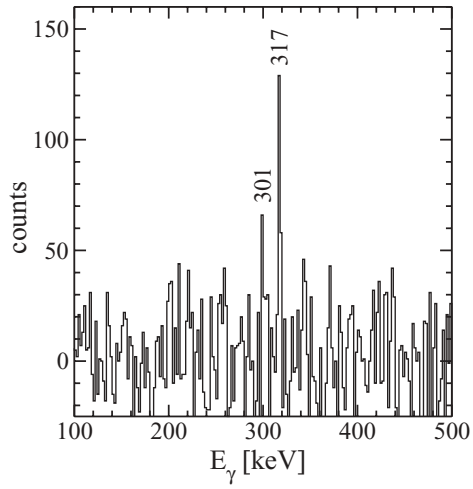

FIG. 3. Low-energy portion of coincidence spectrum double-gated on the 877- and 1814-keV transitions in the PPP data.

exhibited broadening from Doppler shifts, indicating that this state decays faster than the stopping time for the nucleus in the target. Higher-lying transitions are expected to be faster and thus more broadened, making them increasingly difficult to observe above background.

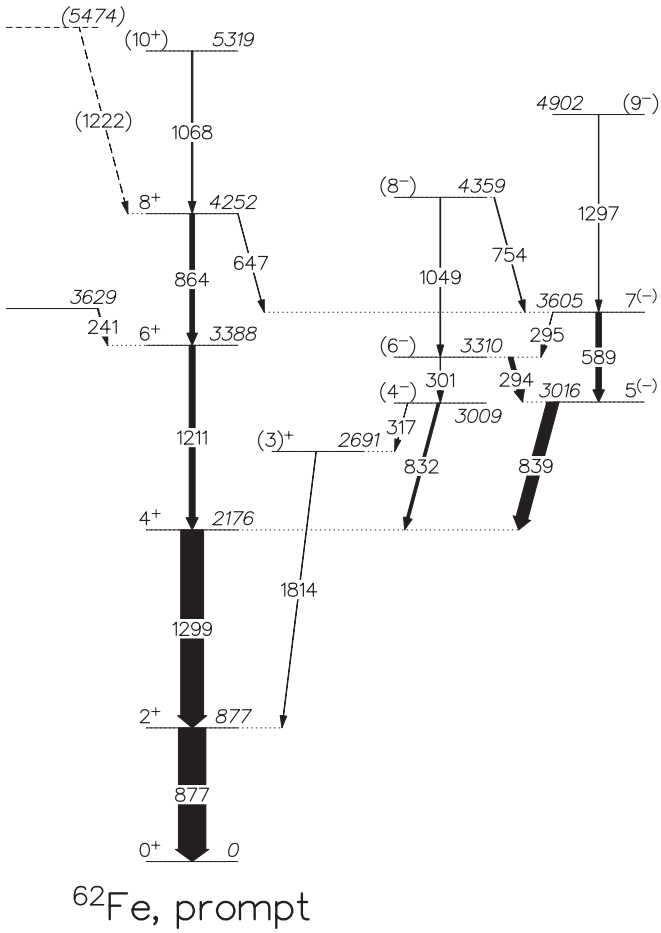

FIG. 4. Level scheme of ^{62}Fe deduced from the PPP data. The widths of the arrows are proportional to the γ-ray intensities.

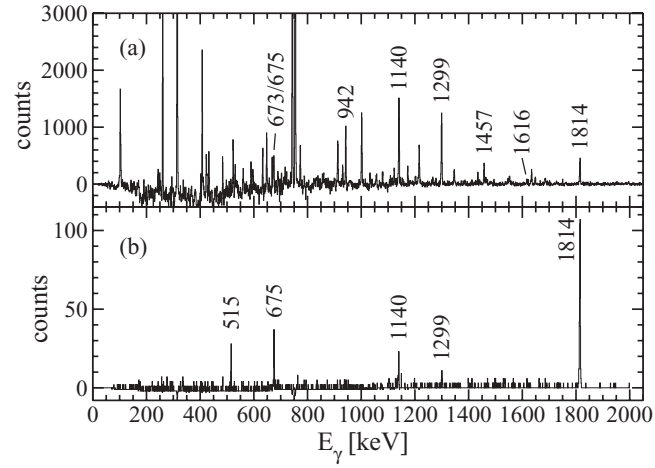

FIG. 5. Coincidence spectra from the DDD data (a) single-gated on the 877-keV transition and (b) double-gated on the 877- and 942-keV transitions. The γ rays assigned to ^{62}Fe are labeled with their energies in keV. In panel (a), the peaks that go off the scale are contaminants.

The γ rays arising from states in ^{62}Fe populated in the β decay of ^{62}Mn isomers are presented in Fig. 5(a) from a single coincidence gate on the 877-keV peak in the DDD cube. The line at 1457 keV proposed by Runte *et al.* [16] is evident, along with a number of γ rays not previously observed. The placement by Runte *et al.* [16] of the 942-keV γ ray depopulating a (0$^+$) level at 1820 keV is inconsistent with the present data: A double gate on the 877- and 942-keV γ rays [Fig. 5(b)] reveals coincident transitions at 515 and 675 keV. These can be placed as depopulating a level at 2691 keV, parallel to the 1814-keV transition, with the ordering of the 1814- and 942-keV γ rays reversed from that of Ref. [16]. Coincidence relationships such as those of Figs. 1(b) and 5 provide the basis for the ^{62}Fe level scheme proposed, in Fig. 6, from the β decay of ^{62}Mn isomers.

The properties of the levels and γ rays assigned to the decay of ^{62}Mn isomers are listed in Table II. The intensities for the four transitions marked with asterisks were derived from comparisons with intensities observed by Hannawald [19] in the β decay of ^{62}Mn at ISOLDE. Owing to the tape cycle used in the latter measurements for collecting sources and counting γ rays, those intensities would be unlikely to include contributions from the 92-ms 1$^+$ isomer proposed by Gaudefroy *et al.* [20]. In addition, as the gate conditions for the DDD cube require three γ rays, transitions to the ground and first-excited states that are not populated from higher-energy levels are not observed.

Liddick *et al.* [12] did not find any evidence for the population of the 4$^+$ level in ^{60}Fe in their study of the decay of the 1$^+$ isomer in ^{60}Mn; analogously, little population of the 4$^+$ level in ^{62}Fe is to be expected in the decay of the 1$^+$ isomer of ^{62}Mn. Therefore, the relative intensities observed in the Gammasphere experiment for decay of the 4$^+$ isomer in ^{62}Mn have been normalized to the value of 38 derived from the ISOLDE data for the 1299-keV 4$^+ \rightarrow$ 2$^+$ transition [19].

TABLE I. Properties of levels and γ rays in ^{62}Fe deduced from the prompt data. The intensities I_γ are normalized to 100 for the 1299.2-keV $4^+ \rightarrow 2^+$ transition. The tentative 1222-keV γ ray and corresponding initial state have been excluded. The angular-correlation coefficients a_2 and a_4 were deduced from a gate on the 1299.2-keV $E2$ transition. The last column gives the γ-ray multipolarities as established for the ^{62}Fe prompt level scheme. $M1$ transitions typically will have some $E2$ admixture.

E_{level} (keV)	I^π	E_γ (keV)	I_γ	a_2	a_4	Multipolarity
877.3	2^+	877.3(1)		0.12(1)	0.03(2)	$E2$
2176.5	4^+	1299.2(1)	100			$E2$
2691.3	$(3)^+$	1814.0(5)	0.7(3)			$\|\Delta I\| = 1\ M1$
3008.9	(4^-)	317.0(4)	0.7(3)			$(\|\Delta I\| = 1\ E1)$
		832.4(2)	8.6(15)	0.18(10)	0.00(15)	$(\Delta I = 0\ E1)$
3015.7	$5^{(-)}$	839.2(1)	51.0(25)	−0.07(2)	0.05(3)	$\|\Delta I\| = 1\ (E1)$
3310.0	(6^-)	294.3(2)	17.0(15)			$(\|\Delta I\| = 1\ M1)$
		301.2(2)	1.9(5)			$(E2)$
3387.8	6^+	1211.3(1)	26.5(15)	0.12(4)	0.01(6)	$E2$
3604.9	$7^{(-)}$	294.8(3)	1.4(5)			$(\|\Delta I\| = 1\ M1)$
		589.2(1)	22.8(12)	0.14(4)	0.05(6)	$E2$
3629.4		241.6(2)	5.0(10)			
4251.7	8^+	647.1(3)	1.2(6)			$\|\Delta I\| = 1\ (E1)$
		863.9(1)	17.8(14)	0.14(5)	0.07(8)	$E2$
4358.7	(8^-)	754.0(2)	1.4(4)			$(\|\Delta I\| = 1\ M1)$
		1048.7(3)	3.2(8)			$(E2)$
4902.0	(9^-)	1297.3(3)	2.4(8)			$(E2)$
5319.4	(10^+)	1067.7(2)	5.1(7)			$(E2)$

B. ^{60}Fe level scheme

In this study, new levels have also been identified in ^{60}Fe that are populated in the decay of the ^{60}Mn isomers. These new data improve upon the previous β-decay scheme of Norman *et al.* [11] and complement the full spectrum of ^{60}Fe high-spin levels presented by Deacon *et al.* [15] from data obtained at Gammasphere in a reaction of ^{48}Ca with ^{13,14}C targets. The spectrum in coincidence with a single gate in the

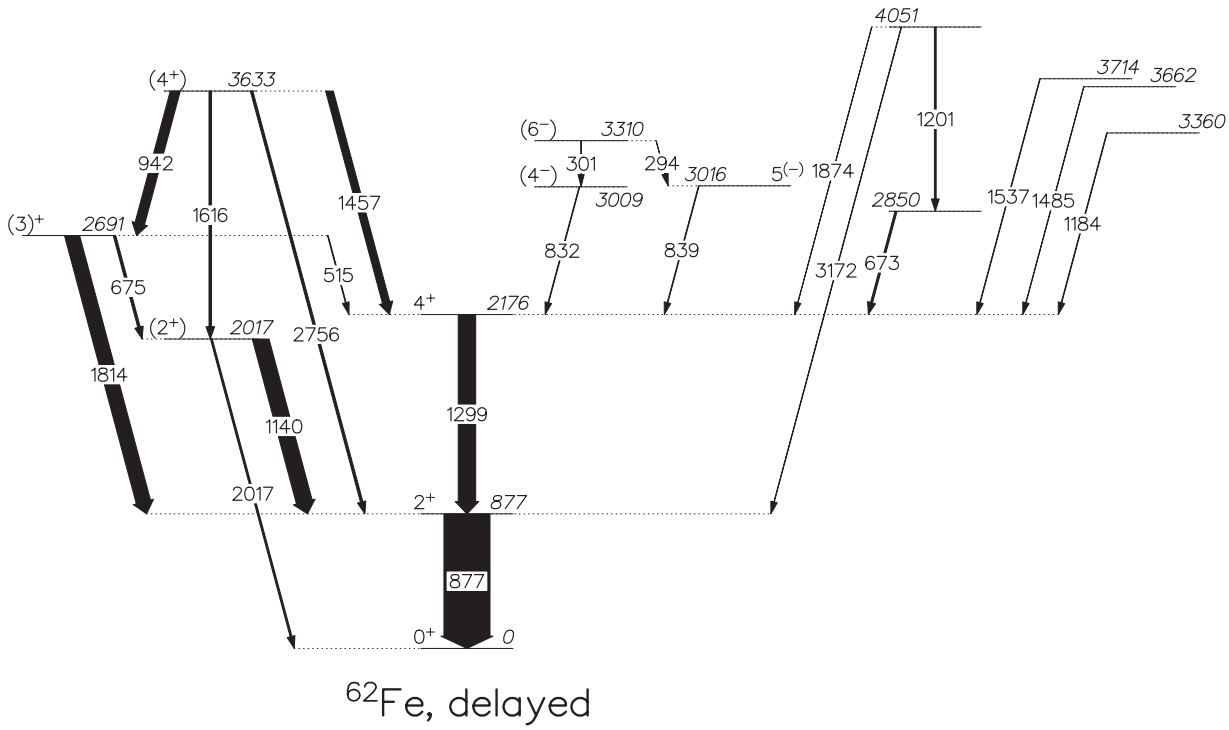

FIG. 6. Level scheme of ^{62}Fe deduced from the DDD data. The widths of the arrows are proportional to the γ-ray intensities.

TABLE II. Properties of levels and γ rays in ^{62}Fe from the β decay of isomers in ^{62}Mn, deduced from the delayed data. The intensities I_γ are normalized as described in the text. The angular-correlation coefficients a_2 and a_4 were deduced from a gate on the 877.3-keV $E2$ transition. The last column gives the γ-ray multipolarities as established for the ^{62}Fe delayed level scheme. $M1$ transitions typically will have some $E2$ admixture.

E_{level} (keV)	I^π	E_γ (keV)	I_γ	a_2	a_4	Multipolarity
877.3	2^+	877.3(1)	100*			$E2$
2017.1	(2^+)	1139.8(2)	35(3)			$(\Delta I = 0\ M1)$
		2017.0(10)	4.0(20)			$(E2)$
2176.5	4^+	1299.2(1)	38.0*	0.06(7)	0.10(10)	$E2$
2691.3	$(3)^+$	515.2(2)	1.6(4)			$\lvert\Delta I\rvert = 1\ M1$
		674.8(2)	5.4(8)			$(\lvert\Delta I\rvert = 1M1)$
		1814.0(2)	31.9(25)	−0.38(9)	−0.14(12)	$\lvert\Delta I\rvert = 1\ M1$
2849.8		673.3(2)	4.4(8)			
3008.9	(4^-)	832.4(5)	1.5(5)			$(\Delta I = 0\ E1)$
3015.7	$5^{(-)}$	839.3(5)	1.5(5)			$\lvert\Delta I\rvert = 1\ (E1)$
3310.0	(6^-)	294.3(5)	0.6(3)			$(\lvert\Delta I\rvert = 1\ M1)$
		301.0(10)	< 0.2			$(E2)$
3360.3		1183.8(15)	1.3(6)			
3633.4	(4^+)	941.8(2)	21.1(15)	0.23(7)	0.00(11)	$(\lvert\Delta I\rvert = 1\ M1)$
		1457.1(2)	16.3(12)			$(\Delta I = 0\ M1)$
		1616.4(3)	5.5(9)			$(E2)$
		2756.0(5)	5.3(7)*			$(E2)$
3661.7		1485.2(15)	0.9(4)			
3713.7		1537.2(15)	1.2(6)			
4050.9		1201.1(3)	3.8(8)			
		1874.0(15)	0.5(5)			
		3172.3(9)	1.0(5)*			

DDD cube on the 824-keV $2^+ \rightarrow 0^+$ transition is presented in Fig. 7(a), along with the double gate on the 1291- and 824-keV $4^+ \rightarrow 2^+ \rightarrow 0^+$ cascade in Fig. 7(b). Coincidence relationships such as these form the basis for the proposed ^{60}Fe level scheme from the decay of the high-spin 4^+ isomer in ^{60}Mn; see Fig. 8(a). Properties of the observed γ rays and levels are summarized in Table III.

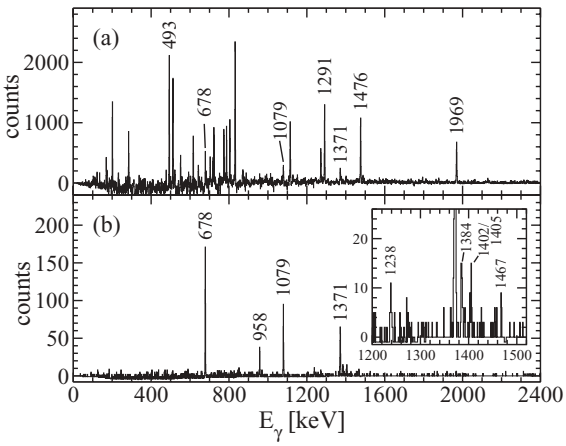

FIG. 7. Coincidence spectra from the DDD data (a) single-gated on the 824-keV transition and (b) double-gated on the 824- and 1291-keV transitions. The γ rays assigned to ^{60}Fe are labeled with their energies in keV. The inset shows a portion of the same spectrum as in (b) on an expanded scale.

The 1402-, 1405-, and 1467-keV transitions marked in the inset of Fig. 7(b) have not been placed in the ^{60}Fe delayed level scheme [Fig. 8(a)]. Intense γ rays with these energies were observed by Deacon *et al.* [15], as well as in the prompt data of the present work, to feed the 2115-keV 4^+ state from levels with spins 5 and 6. The latter could be indirectly populated in the β decay of ^{60}Mn through unidentified higher-energy levels, or these lines may be from a small fraction of the prompt decays for these strong lines appearing in the delayed time gate. In contrast, the weak 1238- and 1384-keV delayed γ rays were not observed in the prompt data and were placed in the delayed level scheme.

All states below 3.1 MeV identified in the current work had been observed in previous β-decay studies. Furthermore, the levels identified here in the DDD data at 3072 and 3499 keV were also populated via $L = 4$ transfer in a (t, p) reaction [13], whereas those proposed at 3193, 3353, and 3486 keV are new. A level at 3293(4) keV was identified in the (t, p) reaction with a sizable cross section and an L value of 3, indicating spin and parity of 3^-. Comparisons of the energies reported in the (t, p) [13] and $(t, p\gamma)$ [23] reactions suggest that discrepancies of up to 15 keV in the level energies may be present in the former. In the $(t, p\gamma)$ reaction, a state has been reported at 3307.7 keV that decays to 2^+ levels at 824 and 2673 keV, and it appears likely to be the 3^- state. There is no evidence for either direct or indirect population of this 3307.7-keV level nor any state in the energy range from 3307.7 down to 3290 keV in the current study. Moreover, there is also no indication for the

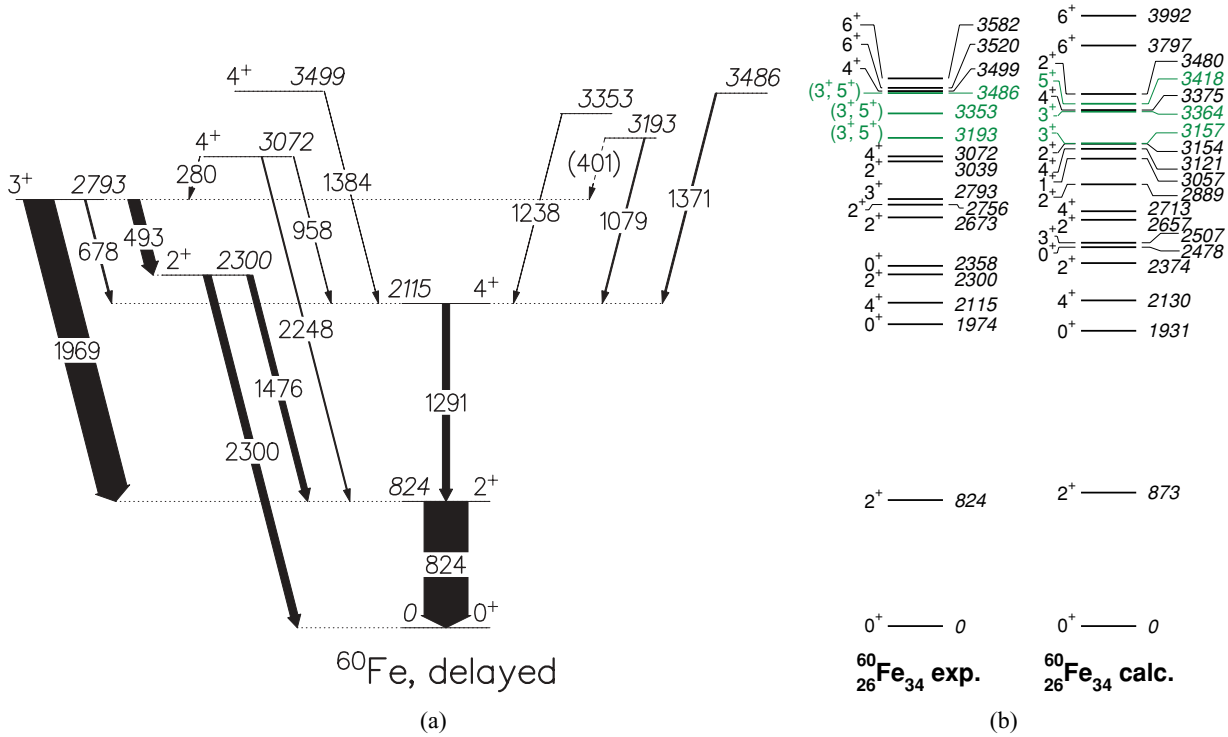

FIG. 8. (Color online) (a) Level scheme of ^{60}Fe deduced from the DDD data. The widths of the arrows are proportional to the γ-ray intensities. (b) Experimental and calculated spectra of positive-parity states in ^{60}Fe. In the online version, the new experimental $(3^+,5^+)$ levels and their corresponding calculated states are in green. See text for details.

direct or indirect population of other 2^+ levels identified in the (t,p) and $(t,p\gamma)$ reactions at 2673, 2756, and 3039 keV that decay to the 824-keV 2_1^+ level by 1849-, 1932-, and 2215-keV γ rays, respectively.

C. Spin and parity assignments

Included in Tables I, II, and III are the results of angular-correlation analyses using the techniques described by Hoteling *et al.* [22]. The time conditions used to create

TABLE III. Properties of levels and γ rays in ^{60}Fe from the β decay of isomers in ^{60}Mn, deduced from the delayed data. The intensities I_γ are normalized to 100 for the 823.8-keV $2^+ \rightarrow 0^+$ transition. The angular-correlation coefficients a_2 and a_4 were deduced from a gate on the 823.8-keV $E2$ transition. The last column gives the γ-ray multipolarities as established for the ^{60}Fe delayed level scheme. $M1$ transitions typically will have some $E2$ admixture.

E_{level} (keV)	I^π	E_γ (keV)	I_γ	a_2	a_4	Multipolarity
823.8	2^+	823.8(1)	100*			$E2$
2114.6	4^+	1290.8(1)	16.4(8)	0.17(7)	0.05(9)	$E2$
2299.6	2^+	1475.8(1)	13.8(7)	−0.18(7)	0.4(1)	$\Delta I = 0$ $M1$
		2299.7(2)	17.4(12)			$E2$
2792.7	3^+	493.0(1)	26.2(20)			$\lvert\Delta I\rvert = 1$ $M1$
		678.1(1)	3.6(4)			$\lvert\Delta I\rvert = 1$ $M1$
		1968.8(1)	67.2(34)	−0.22(4)	−0.02(5)	$\lvert\Delta I\rvert = 1$ $M1$
3071.9	4^+	279.6(7)	0.3(2)			$\lvert\Delta I\rvert = 1$ $M1$
		957.5(3)	1.3(2)			$\Delta I = 0$ $M1$
		2248.0(3)	2.4(4)			$E2$
3193.5		401.0(10)	0.2(2)			
		1078.9(2)	2.9(4)			
3352.9		1238.3(5)	0.7(3)			
3486.0		1371.4(2)	3.6(4)			
3498.6	4^+	1384.0(10)	0.5(5)			$\Delta I = 0$ $M1$

the coincidence cubes were also employed to generate prompt and delayed angular-correlation matrices. When gated by a stretched-$E2$ γ ray, the angular-correlation coefficients a_2 and a_4 are expected to be, respectively, 0.10 and 0.009 for a stretched-$E2$ transition and -0.07 and 0.00 for a stretched-$E1$ transition. Arguments for the spin and parity assignments adopted for the ^{60,62}Fe level schemes, based on the measured angular correlations, observed decay patterns, and the existing literature, are presented in the following sections.

1. Assignments in the prompt ^{62}Fe level scheme

The angular-correlation values in Table I for ^{62}Fe are derived from a single gate set in the prompt coincidence matrix on the (assumed pure $E2$) 1299-keV $4^+ \rightarrow 2^+$ transition. $E2$ multipolarity is deduced for the 589-, 864-, 877-, and 1211-keV γ rays and $|\Delta I| = 1$ $E1$ or $M1$ character for the 839-keV transition. These values support the proposed spin and parity assignments for the positive-parity yrast levels through 8^+, as well as spins 5 and 7 for the states at 3016 and 3605 keV, respectively (see Fig. 4). The 5319-keV state is assumed to correspond to the extension of the ground-state band and is tentatively assigned $I^\pi = (10^+)$.

Tentative spin and parity of (4^-) are proposed for the level at 3009 keV in ^{62}Fe on the basis of the following considerations: (1) The angular-correlation value of $a_2 = 0.18(10)$ in the prompt matrix for the 832-keV transition to the 2176-keV 4^+ state excludes a 5^- assignment and is consistent with the value of $a_2 = 0.20$ that would be expected for a $4^- \rightarrow 4^+ \rightarrow 2^+$ cascade; (2) the presence in the prompt data of the 317-keV transition to the $(3)^+$ level at 2691 keV (see Sec. IV C2) excludes a 6^+ assignment; and (3) the absence of any crossover transition to the 877- and (in the delayed data) 2017-keV 2^+ levels suggests a spin greater than 3. A mixed $M1/E2$ multipolarity for the 832-keV transition, with a corresponding 4^+ or 5^+ assignment for the 3009-keV state, cannot be ruled out based on these arguments. However, in Ref. [15], the strongly populated, near-yrast level structure observed above the 3516-keV spin $I = 5$ state in ^{60}Fe was tentatively assigned negative parity. The structure in the prompt ^{62}Fe decay scheme associated with the 3016-keV $5^{(-)}$ state (see Fig. 4) is analogous to that found in ^{60}Fe by Deacon *et al.* [15]: a low-lying sequence of presumed $M1/E2$ transitions with $E2$ crossovers found to have a strong $5^{(-)} \rightarrow 4^+$ decay to the ground-state band. Thus, negative parity is tentatively assigned to this structure in ^{62}Fe, with spins as indicated in Fig. 4.

2. Assignments in the delayed ^{62}Fe level scheme

The angular-correlation values in Table II for ^{62}Fe are derived from a single gate placed on the 877-keV $2^+ \rightarrow 0^+$ transition in the delayed coincidence matrix. The large negative a_2 value of $-0.38(9)$ for the 1814-keV transition to the 877-keV 2^+ state excludes both a 4^+ and a 3^- assignment for the 2691-keV level. Moreover, the largest negative value permitted for a $2^+ \rightarrow 2^+ \rightarrow 0^+$ cascade is -0.314 for a mixing ratio δ of 1.5, whereas large negative values are found for a wide range of δ values for a $3^+ \rightarrow 2^+ \rightarrow 0^+$ cascade. As, in addition, the gate on the 942-keV γ ray (see Fig. 6) does not provide any indication for the direct transition to the ground state that would be expected from a 2^+ level, a spin and parity of $(3)^+$ are assigned to the 2691-keV state (see also Fig. 4).

Quantum numbers $I^\pi = (2^+)$ were adopted for the 2017-keV level in Refs. [24,25] under the assumption that this state is a member of a two-phonon multiplet. The present analysis does not provide any additional information about this state, but the (2^+) assignment is consistent with the decay patterns observed in this work and has been adopted in the level scheme.

The intense decay branches from the level at 3633 keV to the $(3)^+$ and 4^+ states at 2691 and 2176 keV, respectively, relative to the higher-energy crossover transitions to the 2017- and 877-keV 2^+ levels, support the preference for a proposed (4^+) assignment for the 3633-keV state.

The 3009-, 3016-, and 3310-keV levels are common to both the prompt and delayed ^{62}Fe level schemes. The justification for the respective (4^-), $5^{(-)}$, and (6^-) assignments is given in Sec. IV C1.

The five new ^{62}Fe levels proposed at 2850, 3360, 3662, 3714, and 4051 keV (Fig. 6) appear to be directly populated in the β decay of the 4^+ ^{62}Mn isomer, suggesting a 3^+, 4^+, or 5^+ assignment for each. The 4051-keV state additionally decays by a 3172-keV γ ray to the 2^+ level, likely ruling out 5^+ for this state. These assignments are somewhat speculative when one considers the possibility of weak feeding from multiple higher-lying states because of the large Q value of the decay. Consequently, these spins and parities are not labeled on Fig. 6. They are, however, used with tentative assignments in later discussion (Sec. V).

3. Assignments in the delayed ^{60}Fe level scheme

As noted in Sec. IV B, all states below 3.1 MeV identified in the present study have been observed previously. Spin and parity assignments have been adopted for all of these, as well as for the 3499-keV level, in the compilation of Ref. [26]. These assignments were adopted here as well [Fig. 8(a)], with the exception of that for the 2793-keV state, as discussed in the next paragraph.

In the initial study of the β decay of the ^{60}Mn 4^+ isomer, Norman *et al.* [11] proposed spin and parity $(3)^+$ for a strongly populated level at 2792 keV that decays via a 1969-824-keV cascade.[1] Wilson *et al.* [18] subsequently observed population of this level in a reaction similar to the one used in the present study and proposed 4^+ for the spin and parity of this same level, although without supporting arguments. The a_2 and a_4 coefficients for the 1969-824-keV cascade have been determined to be $-0.22(4)$ and $-0.02(5)$, respectively. The large negative value for a_2 rules out a stretched $4^+ \rightarrow 2^+ \rightarrow 0^+$ cascade and supports the 3^+ assignment for the 2793-keV state in ^{60}Fe.

[1] In Ref. [11], the isomer in ^{60}Mn was assumed to have $I^\pi = 3^+$. Their arguments for the $(3)^+$ assignment for the 2792-keV state in ^{60}Fe are unaffected by the change to a 4^+ isomer in ^{60}Mn.

Spin and parity assignments for the three new ^{60}Fe levels proposed at 3193, 3353, and 3486 keV [Fig. 8(a)] follow similar arguments to those in ^{62}Fe discussed at the end of Sec. IV C2: They appear to be directly populated in the β decay of the 4^+ ^{60}Mn isomer but were not populated in the (t,p) reaction, which favors levels with natural parity [$\pi = (-1)^I$], suggesting 3^+ or 5^+ quantum numbers for these three levels. As with ^{62}Fe, these somewhat speculative assignments are not indicated on the level scheme, but they are used tentatively in comparison with calculations and systematics.

The absence of direct, or even indirect, population of the three 2^+ levels at 2673, 2756, and 3039 keV identified in the (t,p) reaction is consistent with the 4^+ assignment for the high-spin isomer in ^{60}Mn. However, decay branches from the other observed 3^+ and 4^+ states are possible, and these should be observed, if present, owing to the requirement of a triple coincidence cascade. Nonetheless, double gates on the 824/1476-keV and 824/1969-keV pairs did not reveal peaks of any significance in the energy range expected for decay of these 2^+ levels, nor were any peaks at the appropriate energies found in the single gate on the 824-keV $2^+ \rightarrow 0^+$ transition. The conclusion must be that the β decay of the 4^+ isomer in ^{60}Mn proceeds very strongly to the proposed 3^+ and 4^+ levels at 2793 and 2115 keV, respectively, with weaker branches to five additional states above 3 MeV.

V. DISCUSSION

Select levels of the even-even $^{54-64}$Fe$_{28-38}$ isotopes are compared in Fig. 9. The lower-spin levels for ^{56,58,60}Fe have been chosen to include states with firm spins and parities, particularly the 0^+, 2^+, and 4^+ levels that lie below the first 6^+ state, with assignments supported by data from both (t,p) reactions and radioactive decay. Usually, there are two 0^+ levels, four or five 2^+ states, one 3^+ level, and two or three 4^+ states. The negative-parity yrast levels shown are all located above the first 4^+ state. Only the three lowest firmly assigned 6^+ levels reported by Deacon *et al.* [15] are shown for ^{60}Fe, along with tentative 7^-, 8^-, and 9^- states and established 8^+ and 10^+ levels. It is important to note that the proposed 8^- level at 5006 keV is not a candidate for an 8^+ assignment as it only decays to proposed 6^- and 7^- states, but not to any of the 6^+ levels reported by Deacon *et al.* [15].

Several features stand out. The narrow energy range as a function of N for the yrast 2^+, 4^+, 6^+ and 8^+ levels in ^{56,58,60}Fe$_{30,32,34}$ can be attributed to the degree to which the configurations of these states are dominated by $(\pi f_{7/2})^{-2}$ excitations. The two 8^+ states found at nearly constant, high energies in ^{56,58,60}Fe are reproduced well by calculations restricted to a pf space for neutrons [28]; as ^{56}Fe has only two valence proton holes and two valence neutron particles, these 8^+ levels appear to correspond to seniority-4 states involving an aligned broken $\pi f_{7/2}$ pair and an aligned broken $\nu p_{3/2}$ pair, with minimal admixture of the higher-energy $(\nu g_{9/2})^2_{8+}$ state. The decrease by more than 1 MeV in the energy of the 8^+ level, from 5333 keV in ^{60}Fe to 4252 keV in ^{62}Fe, can then be interpreted as a direct consequence of the movement of the Fermi surface beyond the $p_{3/2}$ and $p_{1/2}$ orbitals into the region where the $f_{5/2}$ and $g_{9/2}$ orbitals can be occupied as the oscillator-shell boundary at $N = 40$ is approached. In contrast, the positions of the negative-parity 5^- and 7^- levels require the presence of one neutron in the positive-parity $\nu g_{9/2}$ orbital, even in ^{56}Fe. As the Fermi surface moves up steadily as neutrons are added, the negative-parity levels decrease in energy smoothly for all of these nuclei, whereas perturbations of the positive-parity yrast levels are observed only beyond $N = 34$.

McGrory and Raman [28] performed shell-model calculations for ^{56,58,60}Fe using pf-shell neutrons and six $f_{7/2}$ protons with considerable success for the states in all three nuclei. Figure 8(b) provides a summary of observed ^{60}Fe positive-parity levels below 3.5 MeV from the current data, plus those from the ^{58}Fe$(t,p)^{60}$Fe and ^{58}Fe$(t,p\gamma)^{60}$Fe reactions [13,23], in comparison with the positive-parity levels from Ref. [28] up to 3.5 MeV. Two 6^+ states above 3.5 MeV from both the experiment and the calculations are also included in the figure. The success of the calculations is enhanced by the possible identification in the present study of three new (3^+, 5^+) levels in ^{60}Fe that are quite close in energy to calculated states with those spins and parities. These new states now bring the calculated and observed levels below 3.5 MeV into a near one-to-one correspondence [see Fig. 8(b)].

Yrast levels for ^{60,62}Fe were also calculated using the methods described in Refs. [2,29]. Results are provided in Fig. 10 alongside the corresponding data. The shell-model calculations used as input an effective interaction derived using many-body perturbation theory to third order, with folded diagrams summed to infinite order (see Ref. [30] for technical details). The short-range part of the nucleon-nucleon interaction was renormalized via a Green's-function technique, the so-called G-matrix approach [30]. For the nucleon-nucleon interaction, we employed the N3LO interaction model of Entem and Machleidt [31]. The nucleus ^{48}Ca was used as a closed-shell core, with single-particle states in the pf shell for protons and the single-particle states $0f_{5/2}$, $1p_{3/2}$, $1p_{1/2}$, and $0g_{9/2}$ for neutrons for the calculations labeled $pf(g)$ in Fig. 10. The following truncations were applied: For protons, a maximum of two were allowed in the $f_{5/2}$ orbital and up to six in the $f_{7/2}$ orbital; for neutrons, the $p_{3/2}$ orbitals were frozen as being fully occupied, and a maximum of two neutrons were allowed in the $g_{9/2}$ orbital. (Additional details can be found in Ref. [2].) These calculations are found to be in reasonable agreement with the data. The calculated occupancy for the $g_{9/2}$ neutron orbital is given in parentheses for each level. Also shown for comparison in Fig. 10 are calculations labeled pf, which have the same truncations as the $pf(g)$ calculations, but with no excitations into $g_{9/2}$ neutron orbitals permitted. For ^{62}Fe, the latter calculations exhibit obvious discrepancies for states at higher excitation energies, where the $g_{9/2}$ neutron orbital is expected to play a more important role. Specifically, the effects of $g_{9/2}$ neutron occupancy are apparent for the 6^+ level in ^{62}Fe, with a lesser effect on the 4^+ state and almost no effect on the 2^+ state.

Negative-parity levels calculated in the truncated $pf(g)$ space used here (not shown in Fig. 10) are in poor agreement with the experimental data. In ^{60}Fe, for example, the predicted

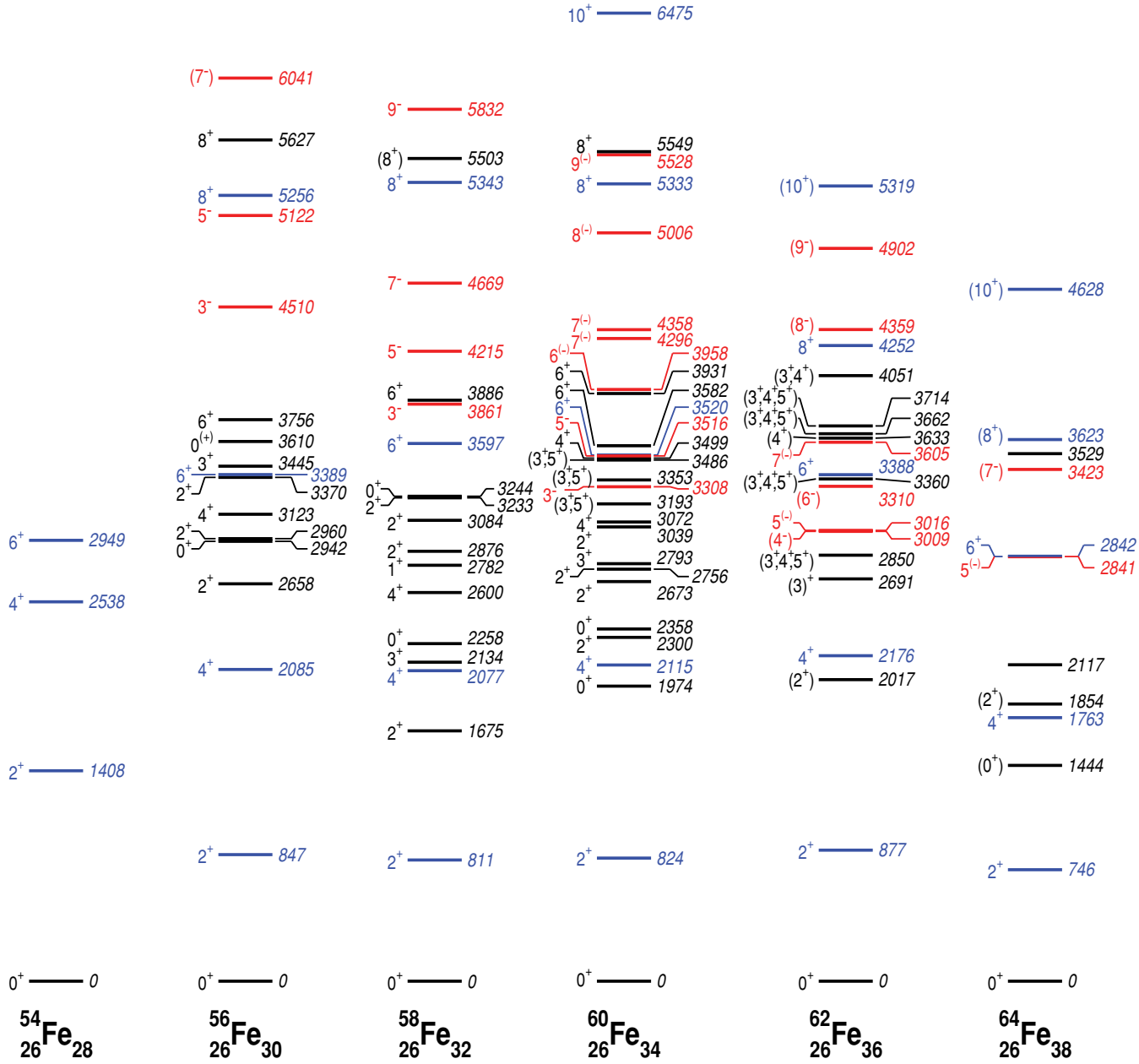

FIG. 9. (Color online) Systematics of levels in the neutron-rich even-even iron isotopes. Data are from Refs. [24,27] for ^{54,56,58}Fe, the current work and Refs. [15,24,26] for ^{60}Fe, the current work for ^{62}Fe, and Refs. [19,22] for ^{64}Fe. See text for details on which levels are included in the figure. In the online version, excited states of the ground-state bands are in blue, and negative-parity levels are in red.

states are generally over 2 MeV too high in energy. Relaxing some of the truncations that were applied and making adjustments to the $g_{9/2}$ neutron single-particle energy, as was done for the calculations in Ref. [22], may improve the agreement somewhat, but such exploration goes beyond the scope of the current work.

Successful descriptions of the observed levels in expanded shell-model calculations should include $g_{9/2}$ valence neutrons and must systematically account for the near constant positions for the 2^+, 4^+, and 6^+ levels through $N = 36$, negative-parity states steadily declining in excitation energy, and the onset of $g_{9/2}$ neutron influence on the location of the 8^+ level in ^{62}Fe$_{36}$ and the 4^+, 6^+, and 8^+ yrast states in ^{64}Fe. It is worth noting that Ljungvall *et al.* [3] performed a recent study of the 2^+ excitation energies and $B(E2;2^+ \rightarrow 0^+)$ strengths for the neutron-rich iron isotopes. They argue that $g_{9/2}$ neutrons have an even larger impact than found here and that the data for the 2^+ states up through $N = 36$ are better reproduced with the inclusion of $g_{9/2}$ neutrons. Beyond $N = 36$, these authors suggest that $d_{5/2}$ neutrons from across the $N = 50$ spherical shell gap start to become important with the development of collectivity as N nears 40. Clearly, further theoretical investigation is required to achieve a full understanding of the available data.

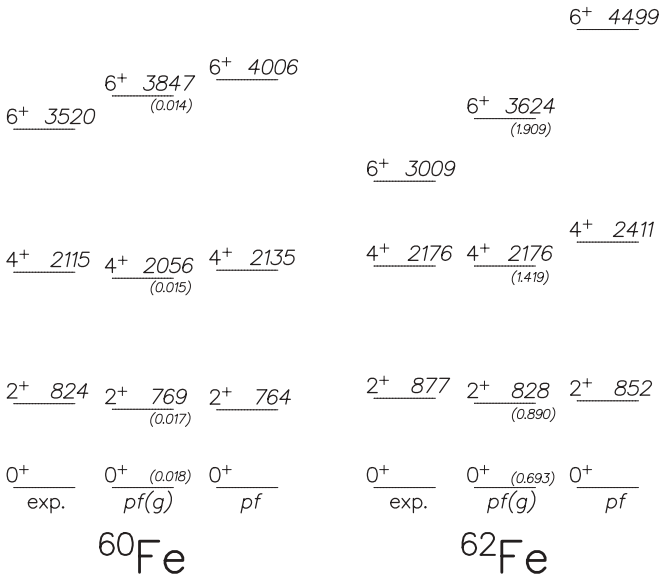

FIG. 10. Experimental and calculated yrast positive-parity levels in ^{60,62}Fe. The labels $pf(g)$ and pf refer to shell-model calculations performed with and without inclusion of $g_{9/2}$ neutrons, respectively. The values in parentheses in the $pf(g)$ sequences give the calculated occupancies of the $g_{9/2}$ neutron orbitals. See text for details.

VI. CONCLUSIONS

In summary, excited states in ^{60,62}Fe were populated both directly in deep-inelastic collisions and by β decay of their ^{60,62}Mn parents. The level schemes of both nuclei from β decay have been extended, as has the high-spin level scheme for ^{62}Fe. Spin and parity assignments could be proposed for some states based on angular-correlation measurements, observed γ-ray decay paths, and comparison with the literature. Systematics of the neutron-rich iron isotopes demonstrate the increasing role of the $\nu g_{9/2}$ orbital as $N = 40$ is approached; this is evidenced by the steadily decreasing energies of the negative-parity levels, which involve at least one $g_{9/2}$ neutron, and by the abrupt decrease in the 8^+ and 10^+ level energies above $N = 34$, in which a pair of $g_{9/2}$ neutrons is involved.

ACKNOWLEDGMENTS

This work was supported in part by the US Department of Energy, Office of Nuclear Physics, under Grant No. DE-FG02-94-ER40834 and Contract No. DE-AC02-06CH11357, and by the Polish Ministry of Science under Contract Nos. 1P03B05929 and NN202103333.

[1] M. Hannawald *et al.*, Phys. Rev. Lett. **82**, 1391 (1999).
[2] N. Hoteling *et al.*, Phys. Rev. C **77**, 044314 (2008).
[3] J. Ljungvall *et al.*, Phys. Rev. C **81**, 061301(R) (2010).
[4] R. Broda *et al.*, Phys. Rev. Lett. **74**, 868 (1995).
[5] O. Sorlin *et al.*, Eur. Phys. J. A **16**, 55 (2003).
[6] A. Gade *et al.*, Phys. Rev. C **81**, 051304(R) (2010).
[7] S. Lunardi *et al.*, Phys. Rev. C **76**, 034303 (2007).
[8] E. Caurier, F. Nowacki, and A. Poves, Eur. Phys. J. A **15**, 145 (2002).
[9] O. Sorlin *et al.*, Phys. Rev. Lett. **88**, 092501 (2002).
[10] Yang Sun, Ying-Chun Yang, Hong-Liang Liu, Kazunari Kaneko, Munetake Hasegawa, and Takahiro Mizusaki, Phys. Rev. C **80**, 054306 (2009).
[11] Eric B. Norman, Cary N. Davids, Martin J. Murphy, and Richard C. Pardo, Phys. Rev. C **17**, 2176 (1978).
[12] S. N. Liddick *et al.*, Phys. Rev. C **73**, 044322 (2006).
[13] D. L. Watson and H. T. Fortune, Nucl. Phys. A **448**, 221 (1986).
[14] W.-D. Schmidt-Ott *et al.*, *Proceedings 6th International Conference on Nuclei Far from Stability and 9th International Conference on Atomic Masses and Fundamental Constants* (Bernkastel–Kues, Germany, 19–24 July 1992), edited by R. Neugart and A. Wöhr, Inst. Phys. Conf. Ser. **132**, 627 (1993).
[15] A. N. Deacon *et al.*, Phys. Rev. C **76**, 054303 (2007).
[16] E. Runte *et al.*, Nucl. Phys. A **399**, 163 (1983).
[17] R. Broda *et al.*, *Proceedings of the International Conference on Fission and Properties of Neutron-Rich Nuclei, Sanibel Island, FL*, edited by J. H. Hamilton and A. V. Ramayya (World Scientific, Singapore, 1998), p. 202.
[18] A. N. Wilson *et al.*, Eur. Phys. J. A **9**, 183 (2000).
[19] M. Hannawald, Ph.D. thesis, Johannes Gutenberg-Universität, Mainz, 2000.
[20] L. Gaudefroy *et al.*, Eur. Phys. J. A **23**, 41 (2005).
[21] I. Y. Lee, Nucl. Phys. A **520**, 641c (1990).
[22] N. Hoteling *et al.*, Phys. Rev. C **74**, 064313 (2006).
[23] E. K. Warburton, J. W. Olness, A. M. Nathan, J. J. Kolata, and J. B. McGrory, Phys. Rev. C **16**, 1027 (1977).
[24] [http://www.nndc.bnl.gov/ensdf].
[25] Huo Junde and Balraj Singh, Nucl. Data Sheets **91**, 317 (2000).
[26] J. K. Tuli, Nucl. Data Sheets **100**, 347 (2003).
[27] Huo Junde and Huo Su, Nucl. Data Sheets **107**, 1393 (2006); Huo Junde, *ibid.* **86**, 315 (1999); M. R. Bhat, *ibid.* **80**, 789 (1997).
[28] J. B. McGrory and S. Raman, Phys. Rev. C **20**, 830 (1979).
[29] N. Hoteling, Ph.D. thesis, University of Maryland, 2008.
[30] Morten Hjorth-Jensen, Thomas T. S. Kuo, and Eivind Osnes, Phys. Rep. **261**, 125 (1995).
[31] D. R. Entem and R. Machleidt, Phys. Rev. C **68**, 041001(R) (2003).